Product Traceability and Uncertainty for the MUSICA ground-based NDACC/FTIR tropospheric H_2O profile product

Version 3

GAIA-CLIM
Gap Analysis for Integrated
Atmospheric ECV Climate Monitoring
Mar 2015 - Feb 2018

A Horizon 2020 project; Grant agreement: 640276

Date: 22 Dec 2017

Dissemination level: PU

Work Package 2; Complied by Matthias Schneider (IMK)

Table of Contents

Version history

Version	Principal updates	Owner	Date
0 draft	First draft	IMK	13.12.2017
1 draft	Minor changes by TG (NPL)	IMK	19.12.2017
2 draft	Minor changes by MS (IMK)	IMK	22.12.2017
3 draft	Minor changes following PT comments	IMK	11.01.2018

1. Product overview

Product name: MUSICA ground-based NDACC/FTIR tropospheric H_2O profile product
Product technique: Remote sensing based on high resolution infrared solar absorption spectrometry
Product measurand: vertical distribution of tropospheric H_2O.
Product form/range: from ground to about 8km (high latitudes) and 12km (low latitudes).
Product dataset: MUSICA ground-based NDACC/FTIR dataset
Site/Sites/Network location: see the following Table 1

Table 1. List of current MUSICA NDACC/FTIR sites (ordered from north to south) and available MUSICA data record. DOFS values report the trace of the averaging kernel matrix. Type 1 is for the tropospheric H2O profile product considered herein, and Type 2 for the isotopologue ratio product HDO/H2O (and the {H2O,δD}-pair product). Adapted from Barthlott et al. (2017).

Site	Location	Altitude	Data record	DOFS (type 1)	DOFS (type 2)
Eureka, Canada	80.1° N, 86.4° W	610 m a.s.l.	2006–2014	2.9	1.7
Ny-Ålesund, Norway	78.9° N, 11.9° E	21 m a.s.l.	2005–2014	2.8	1.6
Kiruna, Sweden	67.8° N, 20.4° E	419 m a.s.l.	1996–2014	2.8	1.6
Bremen, Germany	53.1° N, 8.9° E	27 m a.s.l.	2004–2014	2.8	1.6
Karlsruhe, Germany	49.1° N, 8.4° E	110 m a.s.l.	2010–2014	2.8	1.6
Jungfraujoch, Switzerland	46.6° N, 8.0° E	3580 m a.s.l.	1996–2014	2.7	1.6
Izaña, Tenerife, Spain	28.3° N, 16.5° W	2367 m a.s.l.	1999–2014	2.9	1.7
Altzomoni, Mexico	19.1° N, 98.7° W	3985 m a.s.l.	2012–2014	2.7	1.7
Addis Ababa, Ethiopia	9.0° N, 38.8° E	2443 m a.s.l.	2009–2013	2.6	1.6
Wollongong, Australia	34.5° S, 150.9° E	30 m a.s.l.	2007–2014	2.7	1.6
Lauder, New Zealand	45.1° S, 169.7° E	370 m a.s.l.	1997–2014	2.8	1.6
Arrival Heights, Antarctica	77.8° S, 166.7° E	250 m a.s.l.	2002–2014	2.7	1.4

1.1 Guidance notes

The contribution table to be filled for each traceability contributor has the form seen in Table .

Table 2. The contributor table.

Information / data	Type / value / equation	Notes / description
Name of effect		
Contribution identifier		
Measurement equation parameter(s) subject to effect		
Contribution subject to effect (final product or sub-tree intermediate product)		
Time correlation extent & form		
Other (non-time) correlation		

extent & form		
Uncertainty PDF shape		
Uncertainty & units		
Sensitivity coefficient		
Correlation(s) between affected parameters		
Element/step common for all sites/users?		
Traceable to …		
Validation		

Name of effect – The name of the contribution. Should be clear, unique and match the description in the traceability diagram.

Contribution identifier - Unique identifier to allow reference in the traceability chains.

Measurement equation parameter(s) subject to effect – The part of the measurement equation influenced by this contribution. Ideally, the equation into which the element contributes.

Contribution subject to effect – The top level measurement contribution affected by this contribution. This can be the main product (if on the main chain), or potentially the root of a side branch contribution. It will depend on how the chain has been sub-divided.

Time correlation extent & form – The form & extent of any correlation this contribution has in time.

Other (non-time) correlation extent & form – The form & extent of any correlation this contribution has in a non-time domain. For example, spatial or spectral.

Uncertainty PDF shape – The probability distribution shape of the contribution, Gaussian/Normal Rectangular, U-shaped, log-normal or other. If the form is not known, a written description is sufficient.

Uncertainty & units – The uncertainty value, including units and confidence interval. This can be a simple equation, but should contain typical values.

Sensitivity coefficient – Coefficient multiplied by the uncertainty when applied to the measurement equation.

Correlation(s) between affected parameters – Any correlation between the parameters affected by this specific contribution. If this element links to the main chain by multiple paths within the traceability chain, it should be described here. For instance, SZA or surface pressure may be used separately in a number of models & correction terms that are applied to the product at different points in the processing.

Element/step common for all sites/users – Is there any site-to-site/user-to-user variation in the application of this contribution?

Traceable to – Describe any traceability back towards a primary/community reference.

Validation – Any validation activities that have been performed for this element?

2. Introduction

Most atmospheric molecules interact with electromagnetic radiation in the infrared spectral region, which makes infrared remote sensing an important tool for atmospheric research. High quality solar absorption spectra are measured in the framework of the international networks NDACC (Network for the Detection of Atmospheric Composition Change, https://www2.acom.ucar.edu/irwg) and TCCON (Total Carbon Column Observing Network, http://www.tccon.caltech.edu). NDACC covers the middle infrared spectral range 700 - 4200cm^{-1} and TCCON the near infrared spectral range 3900 - 14000cm^{-1}. The products considered herein were retrieved from NDACC spectra in the 2600 - 3100 cm^{-1} spectral range. The retrievals were performed centrally by the MUSICA NDACC/FTIR retrieval processing approach (the MUSICA activities have been funded by the European Research Council under the European Community's Seventh Framework Programme).

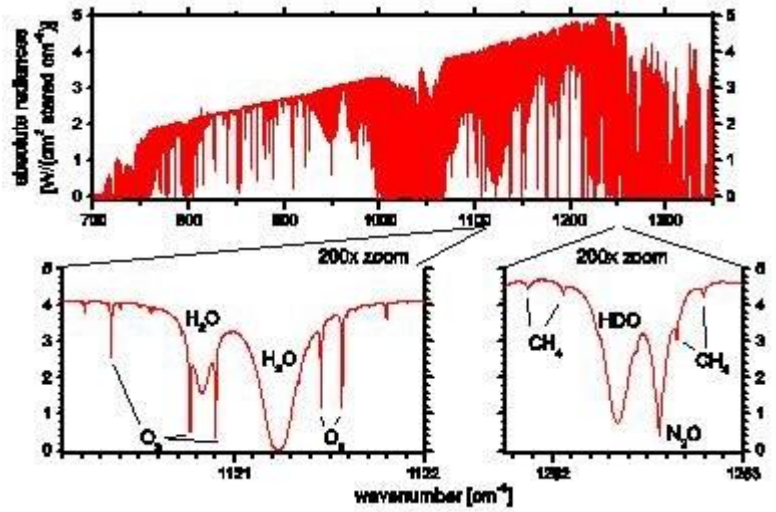

Figure 1. Upper panel: spectrum measured by an NDACC FTIR with the 700 – 1350cm^{-1} filter setting. Bottom panels: zoomed spectral microwindows containing signatures of atmospheric molecules (here H_2O, HDO, O_3, N_2O and CH_4).

Figure 1 shows an example of a spectrum measured in the NDACC spectral region 700 - 1350cm^{-1}. The bottom panel gives an impression of the huge amount of information present in these high resolution spectra. It shows two spectral microwindows with the wavenumber scale being expanded by a factor of 200. Individual rotational-vibrational lines of different absorbers (O_3, H_2O, HDO, N_2O, CH_4, etc.) are discernable. The high spectral resolution allows measurements of the pressure-broadening effect, i.e., the line shape depends on the

pressure at which the absorption takes place (e.g., compare widths of the lines of H_2O, which absorbs mainly in the lower troposphere, with the width of the lines of O_3, which absorbs mainly in the stratosphere). The high resolution spectra disclose not only the total column amount of the absorber but also contain some information about its vertical distribution.

3. Instrument description

Figure 2 shows the two main components of a ground-based FTIR experiment: a precise solar tracker and a high resolution Fourier Transform Spectrometer (FTS). An FTS is based on a Michelson interferometer, consisting of a beamsplitter that divides the incoming radiance into two beams. One of them is reflected by a fixed mirror or retroreflector while the other one is sent to a moving mirror, causing a variable optical path. At the beamsplitter again, they recombine and interfere according to their wavelength and optical path difference. The optical path difference is measured with a monochromatic laser. The observed intensity fluctuations are an interferogram which is converted by a Fourier Transformation into a spectrum. A very detailed description of Fourier transform spectrometry can be found in the textbook of Davis, Abrams and Brault (Davis et al., 2001).

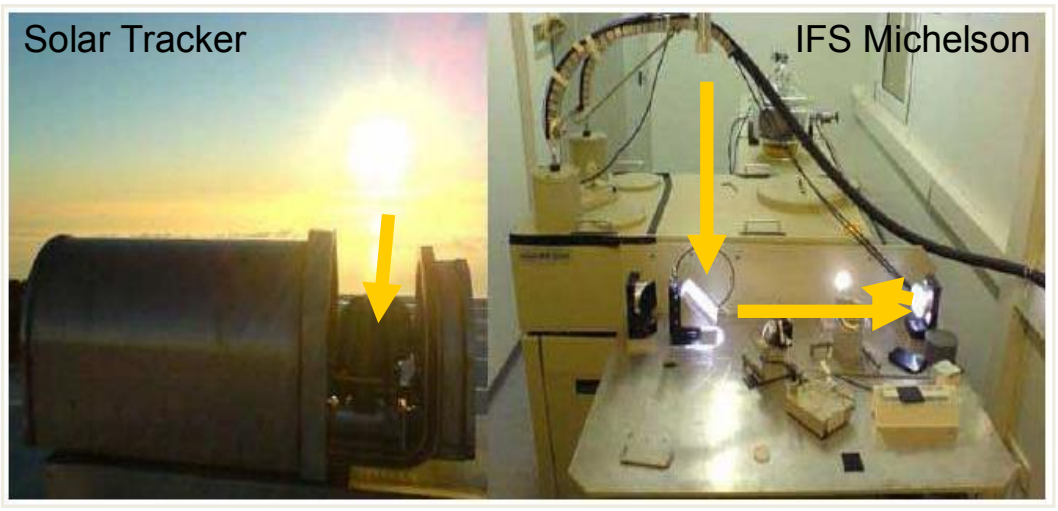

Figure 2. The ground-based FTIR experiment at the Izaña Atmospheric Research Centre. The solar tracker (left photograph) is situated at the top of the experimental housing. It collects the direct solar beam and reflects it into the housing of the FTIR spectrometer (right photograph). Then the solar beam is coupled into the spectrometer (circular light spot on the right part of the photograph).

The physical model chain of the FTIR measurement (Figure 3) displays the physical processes associated with the Fourier transform infrared spectroscopy for atmospheric solar absorption measurements (Figure 4 provides the key for the symbols used). For ground-based FTIR spectroscopy, the primary measurand is the interferogram which is the detected (solar) light intensity against the optical path difference of the moving mirror of a Michelson interferometer setup. Using a fast Fourier transformation (FFT), the interferogram is transformed into an (uncalibrated) transmittance spectrum. Cell spectra are measured in addition to atmospheric spectra. From these dedicated cell measurements, where sharp absorption lines of the gas in the cell (e.g., HBr, N_2O or HCl, at a verified low pressure) are measured, the instrumental line shape (ILS) can be estimated.

Within NDACC, the ILS is then used as an input parameter in the retrieval process, with the purpose of mimicking the instrument's potential small misalignment in the forward model of the radiative transfer in the retrieval software.

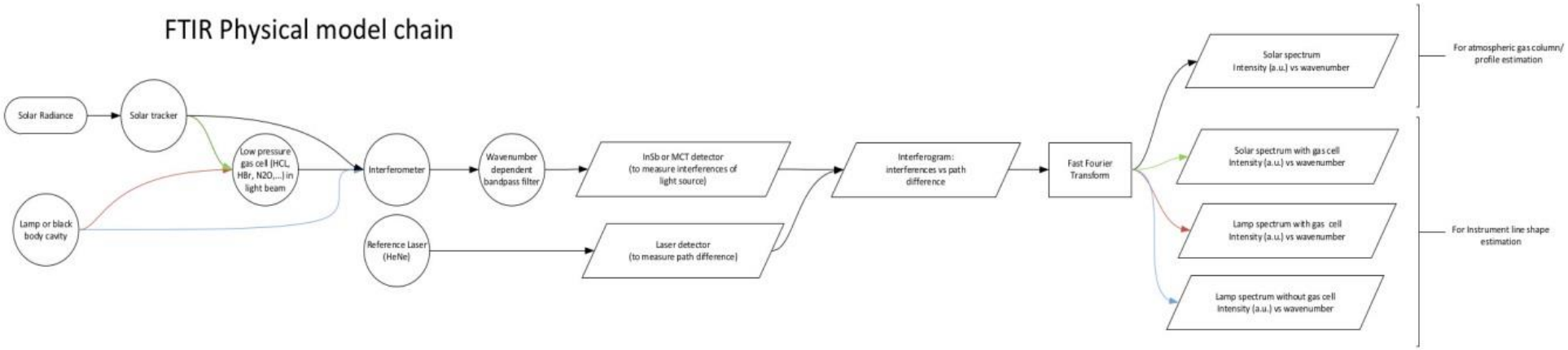

Figure 3. The physical model chain (Measurement Chain).

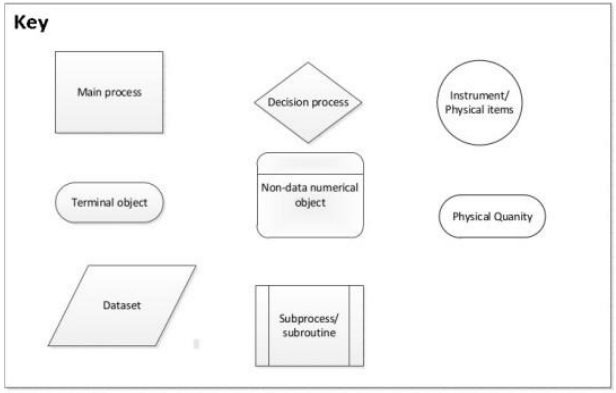

Figure 4. Meaning of the symbols used in the chain figures (Figs. 3, 5 and 6).

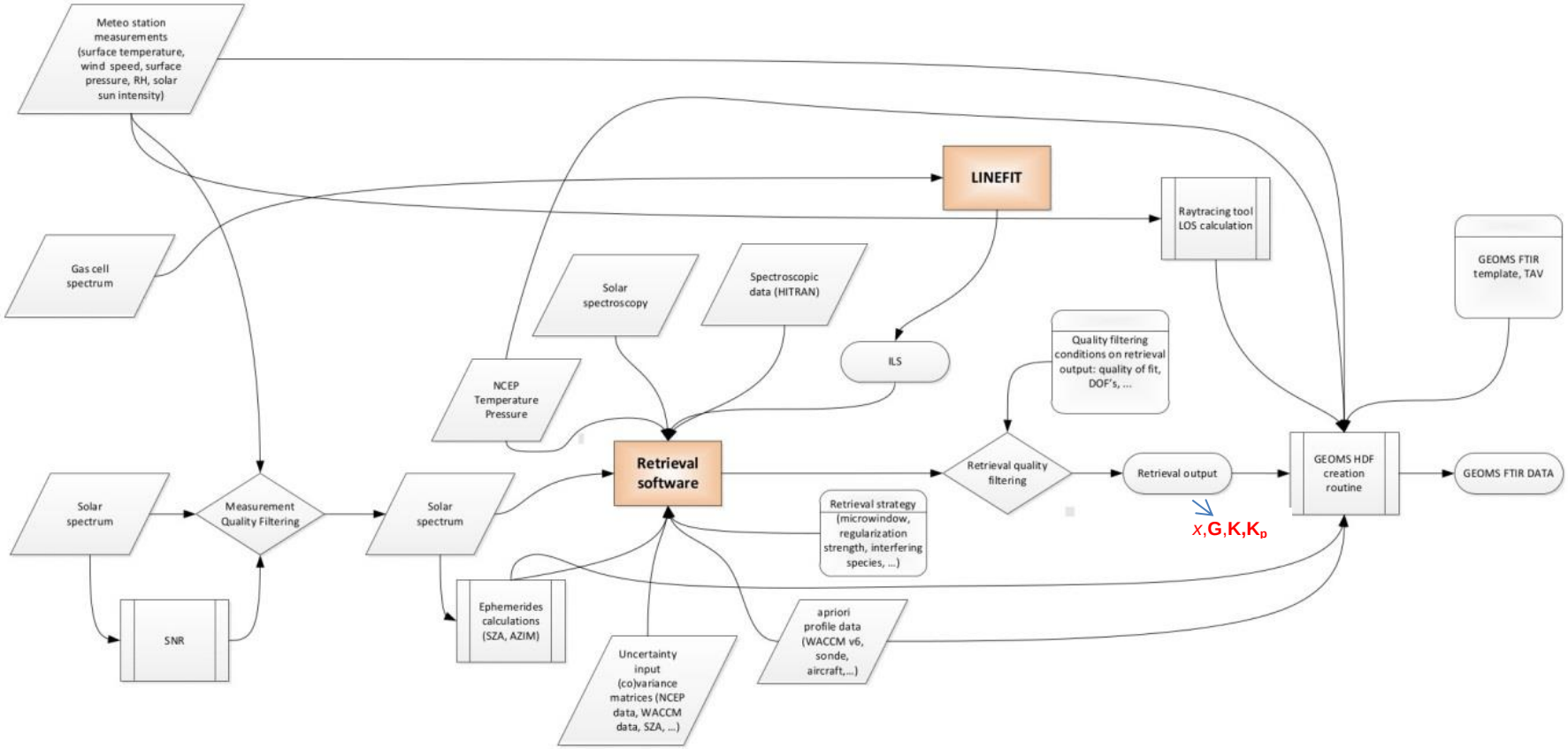

Figure 5. NDACC processing chain (the retrieval output is the trace gas product state vector *x* together with the gain matrix G and the Jacobians K and K_p, which enable to analytically estimate the propagation of the uncertainties into the retrieved state vector).

4. Product Traceability Chain

4.1 Processing chain

The processing chain (Figure 5) display all required *a priori* and input parameters necessary to determine a retrieval of the abundance of a target gas out of an FTIR spectrum. In the NDACC measurements the retrieval software uses optimal estimation or Tikhonov regularization to derive information about the vertical distribution of the target gas in the atmosphere.

All input parameters to the fitting algorithm are provided along with an uncertainty estimate and the retrieval software will propagate all different uncertainty contributions towards the uncertainty on the retrieved concentrations of the target gas. This uncertainty propagation is estimated according to Rodgers (2000), and is possible whenever the retrieval processor outputs the trace gas products together with the gain matrix (**G**) and the Jacobian matrices (**K** and $\mathbf{K_p}$).

4.2 Theoretical background for the processing of FTIR spectra

In the following we give a very brief introduction into the principles of the ground-based FTIR retrieval method. It is an optimal estimation retrieval method and commonly used in atmospheric remote sensing. For more details please refer to Rodgers (2000) and for a general introduction on vector and matrix algebra dedicated textbooks are recommended.

Atmospheric remote sensing means that the atmospheric state is retrieved from the radiation measured after having interacted with the atmosphere. This interaction of radiation with the atmosphere is modelled by a radiative transfer model (also called forward model, *F*), which relates the measurement vector and the atmospheric state vector by:

$$y = F(x, p). \quad (1)$$

We measure *y* (the measurement vector, e.g. a solar absorption spectrum in the case of a ground-based FTIR) and are interested in *x* (the atmospheric state vector). Vector *p* represents auxiliary parameters (like solar elevation angle) or instrumental characteristics (like the instrumental line shape), which are not part of the retrieval state vector. However, a direct inversion of Eq. (1) is generally not possible, because there are many atmospheric states *x* that can explain one and the same measurement *y*.

For solving this ill-posed problem a cost function is set up, that combines the information provided by the measurement with *a priori* known characteristics of the atmospheric state:

$$[y - F(x,p)]^T \mathbf{S_\varepsilon^{-1}} [y - F(x,p)] + [x - x_a]^T \mathbf{S_a^{-1}} [x - x_a]. \quad (2)$$

Here, the first term is a measure of the difference between the measured spectrum (represented by *y*) and the spectrum simulated for a given atmospheric state (represented by

x), while taking into account the actual measurement noise level ($\mathbf{S}_\varepsilon$ is the measurement noise covariance matrix). The second term of the cost function (Eq. 2) constrains the atmospheric solution state (*x*) towards an *a priori* most likely state x_a, where the nature and strength of the constraint are defined by the *a priori* covariance matrix $\mathbf{S_a}$. The constrained solution is reached at the minimum of the cost function (Eq. 2). Due to the nonlinear behaviour of *F(x,p)*, the minimisation is generally achieved iteratively. For the *i+1th* iteration it is:

$$x_{i+1} = x_a + \mathbf{G}_\mathrm{i}[y - F(x_i, p) + \mathbf{K}_\mathrm{i}(x_i - x_a)]. \quad (3)$$

This Eq. (3) is the main measurement equation asked for in the Contributor Table (Table 1). **K** is the Jacobian matrix (derivatives that capture how the measurement vector *y* will change for changes in the atmospheric state *x*) and **G** is the gain matrix (derivatives that capture how the retrieved state vector *x* will change for changes in the measurement vector *y*). **G** can be calculated from **K**, $\mathbf{S}_\varepsilon$ and $\mathbf{S_a}$ as:

$$\mathbf{G} = (\mathbf{K}^\mathrm{T}\mathbf{S}_\varepsilon^{-1}\mathbf{K} + \mathbf{S}_\mathbf{a}^{-1})^{-1}\mathbf{K}^\mathrm{T}\mathbf{S}_\varepsilon^{-1}. \quad (4)$$

The averaging kernel matrix **A** is an important component of a remote sensing retrieval and it is calculated as:

$$\mathbf{A} = \mathbf{GK}\,. \quad (5)$$

The averaging kernel **A** reveals how a small change of the real atmospheric state vector x affects the retrieved atmospheric state vector $\hat{x}$:

$$\hat{x} - x_a = \mathbf{A}(x - x_a)\,. \quad (6)$$

4.3 Propagation of uncertainties

The propagation of parameter uncertainties ε_p can be estimated analytically with the help of the parameter Jacobian matrix $\mathbf{K_p}$ (derivatives that capture how the measurement vector will change for changes in the parameter *p*). According to Eq. (3), using the parameter $p+\varepsilon_p$ (instead of the correct parameter *p*) for the forward model calculations will result in an uncertainty in the retrieved atmospheric state vector x_e of:

$$x_e = -\mathbf{GK_p}\,. \quad (7)$$

The respective uncertainty covariance matrix $\mathbf{S_e}$ is:

$$\mathbf{S_e} = \mathbf{GK_pS_pK_p^TG}^\mathrm{T}\,, \quad (8)$$

where $\mathbf{S_p}$ is the covariance matrix of the uncertainties ε_p.

Noise on the measured radiances also affects the retrievals. The uncertainty covariance matrix for noise can be analytically calculated as:

$$\mathbf{S_e} = \mathbf{GS_yG}^\mathrm{T}, \quad (9)$$

where $\mathbf{S_y}$ is the covariance matrix for noise on the measured radiances *y*.

4.4 Trace gas ratios

The results can also be used to directly estimate the ratio of the concentration of different gases. This is particularly relevant when studying the ratios of different isotopologues of the same gas. By transferring the matrices **G** on the logarithmic scale for the state vector *x*, we can perform an analytical uncertainty estimation of trace gas ratios. The uncertainty covariances for the trace gas ratios are calculated in analogy to Eqs. (8) and (9):

$$\mathbf{S_e} = \mathbf{P}\mathbf{G}_{\log}\mathbf{K_p}\mathbf{S_p}\mathbf{K_p}^{\mathrm{T}}\mathbf{G}_{\log}^{\mathrm{T}}\mathbf{P}^{\mathrm{T}} \quad (10)$$

and

$$\mathbf{S_e} = \mathbf{P}\mathbf{G}_{\log}\mathbf{S_y}\mathbf{G}_{\log}^{\mathrm{T}}\mathbf{P}^{\mathrm{T}}\,, \quad (11)$$

where $\mathbf{G}_{\log}$ is the gain matrix with respect to the trace gas logarithmic scale concentrations of the two trace gases (derivatives that capture how the retrieved logarithmic scale state vectors *x* will change for changes in the measurement vector *y*). The matrix **P** is an operator that realises the transformation on a basis defined as the difference between the logarithmic scale concentrations of the two trace gases, i.e. the logarithmic scale differences between the states of the two trace gases are used as proxy for the trace gas ratios. This method enables calculation of the uncertainties on a gas ratio product, which will generally be less than those for a single gas product.

The averaging kernels for trace gas ratios can be calculated as:

$$\mathbf{P}\mathbf{A}_{\log}\mathbf{P}^{-1}\,, \quad (12)$$

where $\mathbf{A}_{\log}$ is the averaging kernel for the trace gas logarithmic scale concentrations of the two trace gases.

This method for analytically documenting the averaging kernels and the uncertainties of trace gas ratio remote sensing data is used by MUSICA (http://www.imk-asf.kit.edu/english/musica.php) for the HDO/H_2O product. For more details please refer to Schneider et al. (2012) and Barthlott et al., (2017).

4.5 Traceability of uncertainties

The contributing uncertainties of a ground-based FTIR data product are collected in the matrices $\mathbf{S_p}$ (for the uncertainties of the parmeters *p*) and the matrix $\mathbf{S_y}$ (for the noise on the measured radiances). The uncertainties affect the calculations according to Eq. (3) (the "measurement equation"), i.e. the retrieval product. The propagation of the uncertainties into the retrieval product can be calculated according to Eqs. (7) - (11).

In the next Section we present the Contributor Tables (according to Table 2), i.e. we discuss

the traceability of the entries in $\mathbf{S_p}$ and $\mathbf{S_y}$. The following uncertainty contributors from the physical model/measurement chain and from the processing chain represent the major sources of uncertainty, and the contribution of each one is discussed in Section 5.

Uncertainty contributors from the measurement chain:

- A1: White noise in the measured spectral radiances (measurement noise)
- A2: Spectral baseline distortions (due to intensity fluctuations, detector non-linearities and multi-reflections on optical elements)

Uncertainty contributors from the processing chain:

- B1: Line of sight/Pointing
- B2: Instrumental line shape (modulation efficiency and phase error)
- B3: Spectroscopic parameters and parameterisations
- B4: Solar spectroscopy
- B5: Atmospheric temperature profile assumptions

Figure 6 presents a summary of the overall product traceability and uncertainty chain, which effectively combines the physical and processing chains (Figures 3 and 5 respectively), and highlights (in red) where the major uncertainty effects occur within the process. It is assumed that the uncertainty contributions from the other elements in this figure are minor relative to the seven identified above.

It should be noted that the limited vertical resolution and sensitivity of the remote sensing data is not an uncertainty contributor. These limitations are not uncertain, instead they are a fully understood characteristic of the remote sensing data product and comprehensively described by the averaging kernels (see Eqs. 5 and 6). Figure 7 shows a typical averaging kernel for the MUSICA H_2O profile product. Profiling capability is limited to the troposphere.

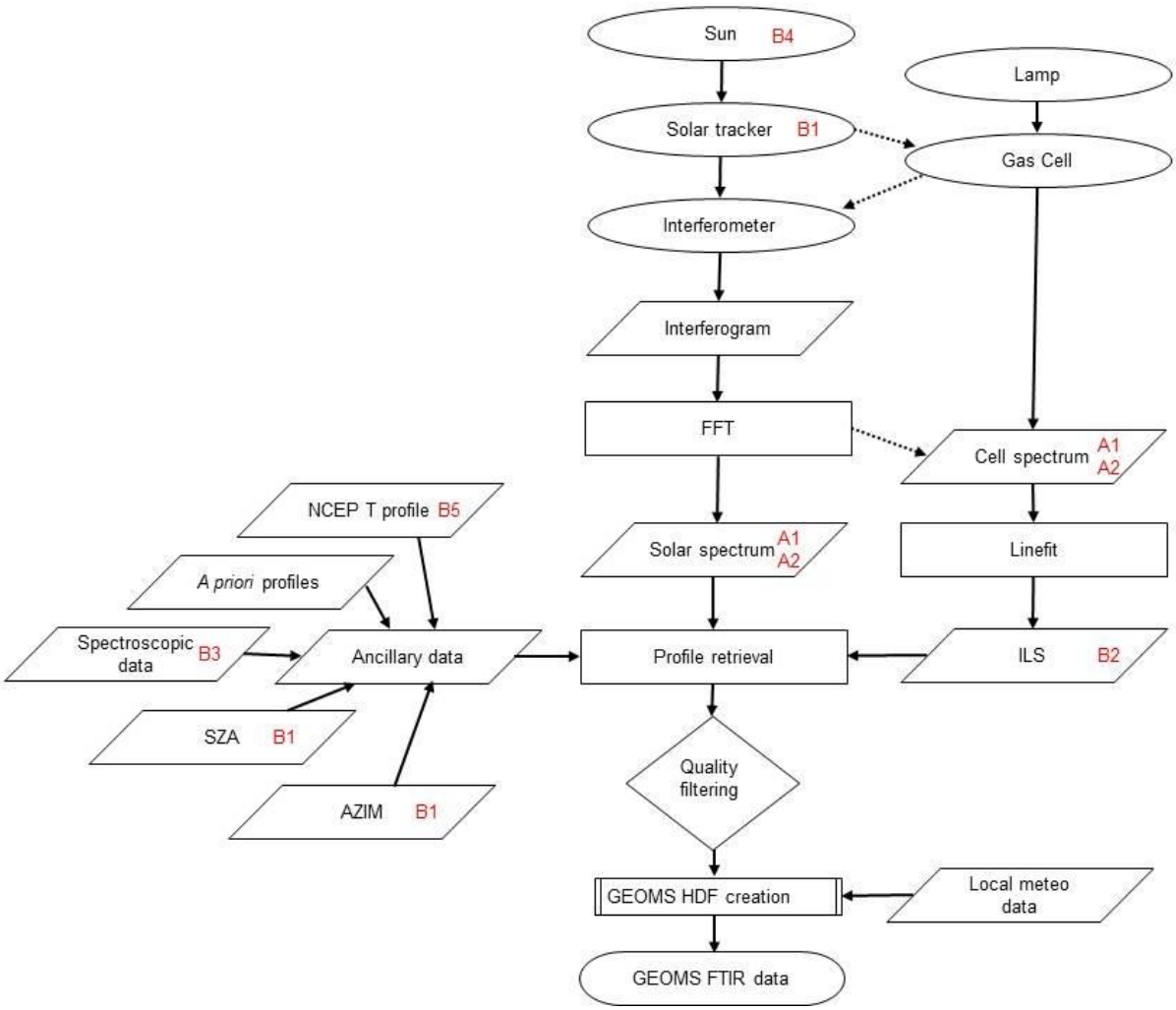

Figure 6. Overall product traceability and uncertainty chain, with key uncertainty contributors highlighted in red text

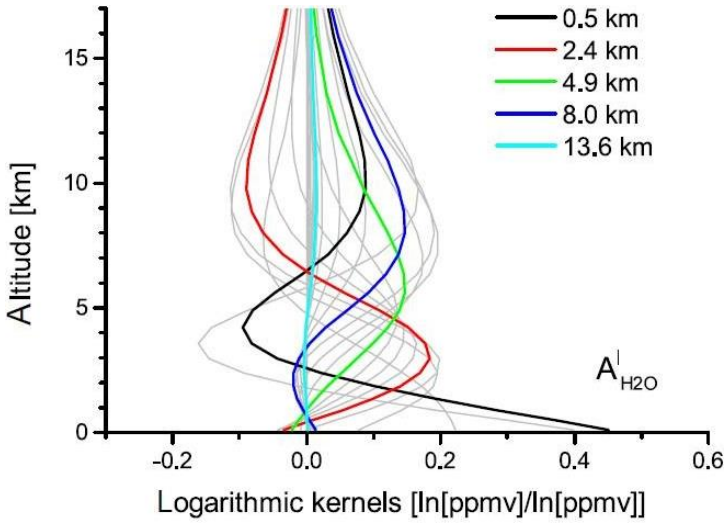

Figure 7. Logarithmic scale averaging kernel for a typical MUSICA H2O profile product (Graphic is adopted from Fig.4 of Barthlott et al., 2017). Negative values mean a negative response, e.g. for the shown example a H2O increase at 2.4 km will negatively affect the H2O concentrations retrieved at 10 km.

5. Element contributions

5.1 Measurement noise (A1)

For the measurement noise covariance matrix $\mathbf{S_y}$ generally a diagonal matrix is assumed. The correct entries for this matrix can be estimated by analysing the noise in a wavelength region of a measured spectrum where no significant atmospheric absorption takes place.

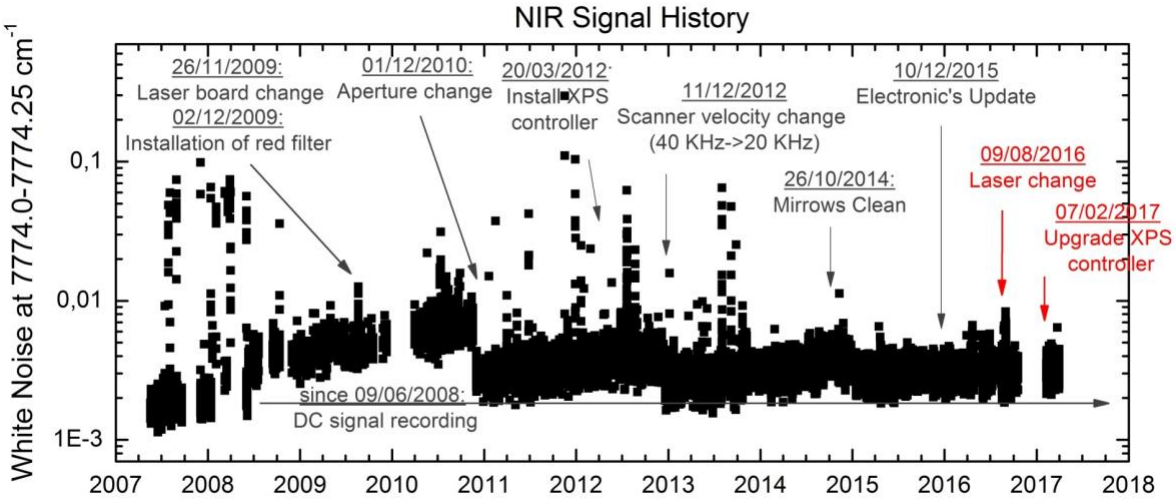

Figure 8. Evolution of the white noise (expressed as noise-to-signal ratio) in the near infrared region of the FTS at the Izaña Atmospheric Research Centre.

Figure 8 shows such analysis for a region in the near infrared. We observe that the noise depends on different instrumental settings, i.e. the entries of $\mathbf{S_y}$ for estimating the uncertainty contribution of measurement noise will be different for different instruments or for different time periods that shall be unique to each instrument and reflect its particular maintenance and component replacement history.

Information / data	Type / value / equation	Notes / description
Name of effect	Measurement noise	
Contribution identifier	A1	
Measurement equation parameter(s) subject to effect	Vector *y* in Eq. (3)	The gain matrix **G**, can also be affected, but only if the actual noise level is used when setting up the retrieval**.**
Contribution subject to effect (final product or sub-tree intermediate product)	Retrieved state vector $\hat{x}$	
Time correlation extent & form	None	No direct time correlation, however amplitude of noise can vary between different

		periods (e.g., by degradation of optical elements, see example of Fig. 8)
Other (non-time) correlation extent & form	None	
Uncertainty PDF shape	Normal	
Uncertainty & units	0.4%, unitless (noise-to-signal ratio)	Typical noise-to-signal ratio in the 2600 - 3100 cm^{-1} spectral range
Sensitivity coefficient	Uncertainty propagation according to Eq. (9)	
Correlation(s) between affected parameters	None	
Element/step common for all sites/users?	Yes	MUSICA processing assumes same uncertainties for all sites. These are conservative assumptions.
Traceable to …	Traceable as shown in Fig. 8.	It is no absolute uncertainty instead it is a relative uncertainty, i.e. the noise is traceable relative to the signal.
Validation	Yes, example see Fig. 8.	

5.2 Spectral baseline distortions (A2)

Intensity fluctuations when recording the interferogram or non-linearities of the detector can cause a baseline distortion of spectrum (a frequency dependent baseline offset).

In addition multi-reflections on optical elements (solar tracker mirrors, beamsplitters, etc.) can cause an artificial channeling signal in the spectrum.

Information / data	Type / value / equation	Notes / description
Name of effect	Baseline distortions	
Contribution identifier	A2	
Measurement equation parameter(s) subject to effect	Affects vector y in Eq. (3)	If known it could be considered in $F(x,p)$. Then it would also affect the gain matrix **G** and the Jacobian matrix **K** in Eq. (3).
Contribution subject to effect (final product or sub-tree intermediate product)	Retrieved state vector $\hat{x}$	

Time correlation extent & form	Structured random	It is usually due to instrumental/hardware problems, that will remain as long as it is not corrected. This shall be instrument and time-period specific
Other (non-time) correlation extent & form		
Uncertainty PDF shape	MUSICA processing assumes 50% random (normal) and 50% systematic.	
Uncertainty & units	<0.2% (baseline-to-signal ratio), unitless	
Sensitivity coefficient	Uncertainty propagation according to Eqs. (7) and (8).	
Correlation(s) between affected parameters	None	
Element/step common for all sites/users?	Yes	MUSICA processing assumes same uncertainties for all sites. These are conservative assumptions.
Traceable to …		It is a relative uncertainty, i.e. it is traceable relative to the signal.
Validation	Laboratory measurements, e.g. Hase (2000).	

5.3 Line of Sight / Pointing (B1)

A mis-pointing of the solar tracker generates a Doppler shift of the solar lines with respect to the telluric spectral features due to the solar rotation. The synodic rotation period of the sun is about 26.75 days, which corresponds to an observed equatorial solar velocity of about 1890ms^{-1} (Gisi et al. 2011 and references therein). A mismatch of the pointing along the solar equator of 1 arc min translates into a Doppler scaling $\Delta\nu/\nu$ of 3.9×10^{-7}. If this effect is considered in the analysis by fitting a separate shift for the solar background lines, the effects on the trace gas analysis are minor, but it gives a useful method to estimate the pointing quality at hand. Note, however, that the exact mispointing cannot be retrieved from the observed Doppler shifts, because there is no sensitivity along the direction parallel to the solar rotation axis. For this reason, we apply an additional factor of $\sqrt{2}$ for estimating the pointing error from the observed solar line scaling (we assume that the pointing uncertainty is of the same size for any direction on the solar disk).

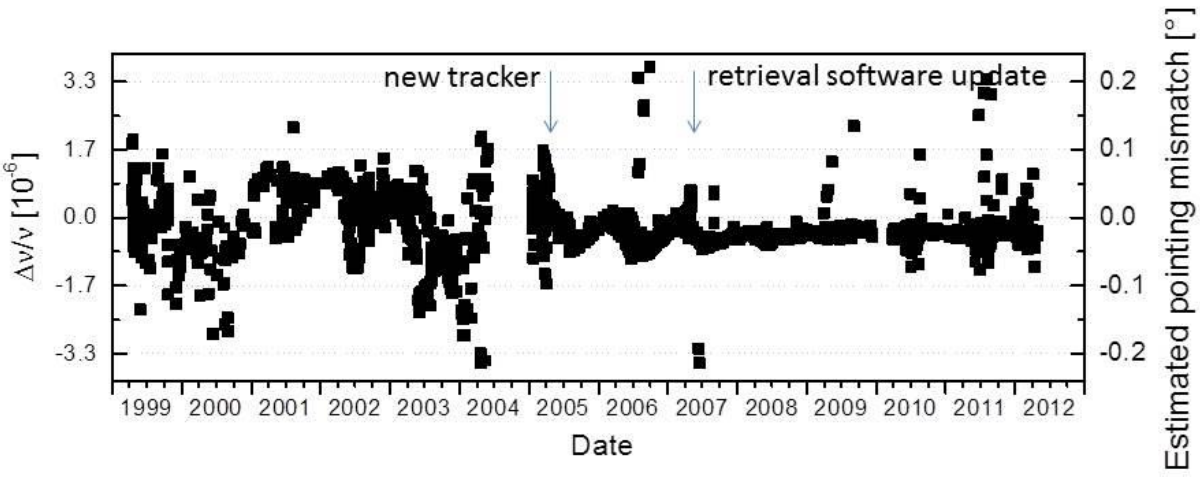

Figure 9. Evolution of solar line shifts and corresponding solar tracker pointing mismatch for the ground-based FTIR instrument of the Izaña Atmospheric Research Centre (example for 1999 - 2012).

Figure 9 shows the evolution of the solar line Doppler scaling and the respectively estimated solar tracker pointing mismatch for the ground-based FTIR experiment of the Izaña Atmospheric Research Centre. Occasionally, we observe some severe mismatch of the pointing, very likely due to the presence of clouds, which disables the camera based tracker's ability to see the sun. These outliers can easily be identified by the solar line shifts. Overall we estimate that with the latest tracker version (in operation since 2005) the pointing mismatch (1σ scatter of the mismatch) is better than 0.002°, which is less than 1% of the radius of the solar disc (the radius of the solar disc is about 0.25°). In the period from 1999 – 2004 (older tracker version), the pointing mismatch was significantly larger. Then the 1σ scatter of the mismatch was 0.04°. In summary the solar tracker pointing mismatch depends on the actual solar tracker used. It can be poorer than 0.05° or as good as about 0.002°.

Information / data	Type / value / equation	Notes / description
Name of effect	Pointing stability	
Contribution identifier	B1	
Measurement equation parameter(s) subject to effect	Affects vector function $F(x,p)$, the gain matrix **G** and and the Jacobian matrix **K** in Eq. (3)	
Contribution subject to effect (final product or sub-tree intermediate product)	Retrieved state vector $\hat{x}$	
Time correlation extent & form	Some time correlation possible (see Fig. 9).	Nature of correlation is site and time-period specific
Other (non-time) correlation extent & form	None	
Uncertainty PDF shape	MUSICA processing assumes 90% of the uncertainty to be random (normal) and the remaining 10% of the uncertainty to be	Barthlott et al. (2017)

	systematic.	
Uncertainty & units	0.1°	Barthlott et al. (2017)
Sensitivity coefficient	Uncertainty propagation according to Eqs. (7) and (8).	
Correlation(s) between affected parameters	Affect the retrieved state vector $\hat{x}$ in the same direction over all altitudes.	Schneider et al. (2012)
Element/step common for all sites/users?	Yes	MUSICA processing assumes same uncertainties for all sites. These are conservative assumptions.
Traceable to …	Qualitatively traceable to solar line frequency shifts (see Fig. 9)	
Validation	Possible, see example and discussion of Fig. 9.	

5.4 Instrumental line shape (B2)

The instrumental line shape (ILS) describes how the FTIR instrument will detect a monochromatic signal. It can be monitored by low pressure cell gas measurements (Hase, 2012). In NDACC this experimentally determined ILS is than used for the trace gas retrieval process.

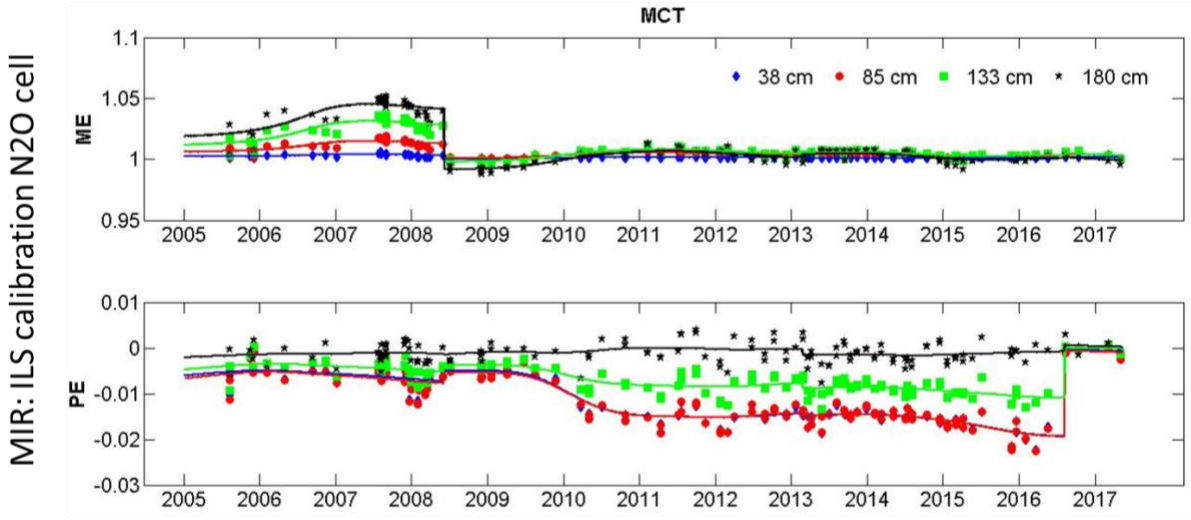

Figure 10. Evolution of the instrumental line shape of the FTS at the Izaña Atmospheric Research Centre (example for the MCT detector branch, 2005 - 2017). Upper panel: Modulation Efficiency (ME); Bottom panel: Phase Error (PE). Dots represent individual cell measurements and the lines the ILS values used when running the retrievals. The different colors represent different optical path differences (OPD): 38 cm, 85cm, 133cm and 180 cm (as given in the legend).

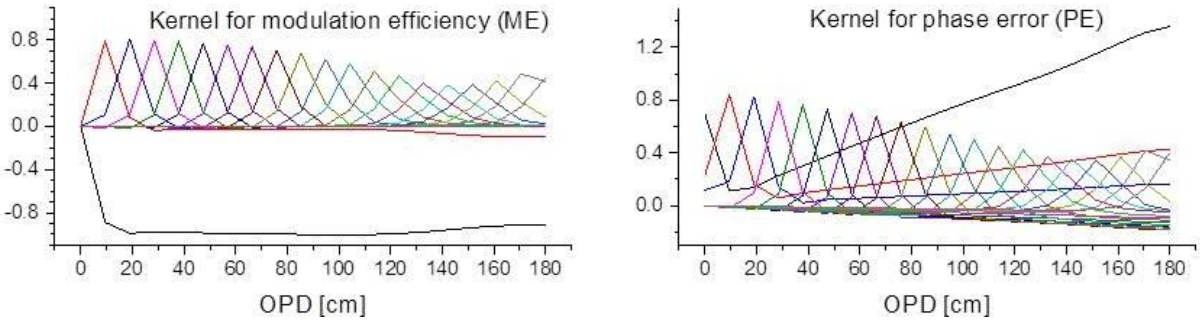

Figure 11. Example of averaging kernels for instrumental line shape retrievals using low pressure N2O cell spectra (shown are results for the FTS at Izaña). The different colours are for 20 equidistant OPDs between 0 and 180cm. Left panel: Modulation Efficiency (ME); Right panel: Phase Error (PE).

Figure 10 shows the evolution of the ILS (modulation efficiency, ME, and phase error, PE) for the FTIR instrument at the Izaña Atmospheric Research Centre. The dots represent individual ILS measurements and the solid line is a smooth line that is fitted to the individual observations. The values given by this smooth line represent most likely the actual ILS, and are the values we use for describing the ILS during the NDACC trace gas retrievals. Thus, the difference of the values on the smooth line and the individual values can be seen as an uncertainty for the most likely ILS values. For the Izaña instrument we can estimate the ILS uncertainty to be smaller than 0.5% (concerning the modulation efficiency) and smaller than 0.003 rad (concerning the phase error). If the nominal ILS is used instead of the retrieved ILS the uncertainties will be larger, respectively.

In order to be able to rely on the ME and PE values obtained from the low pressure gas cell spectra analyses, we must consider the averaging kernels of the respective ME and PE retrievals. Examples for these kernels are shown in Fig. 11. It clearly indicates that the cell measurements allow a reliable retrieval of the ME and PE values over the whole range of OPD (optical path difference).

Information / data	Type / value / equation	Notes / description
Name of effect	Instrumental line shape (ILS)	
Contribution identifier	B2	
Measurement equation parameter(s) subject to effect	Affects vector function $F(x,p)$, the gain matrix **G** and and the Jacobian matrix **K** in Eq. (3)	
Contribution subject to effect (final product or sub-tree intermediate product)	Retrieved state vector $\hat{x}$	
Time correlation extent & form	Structured random	See example of Fig. 10. By nature these will be instrument / site specific.
Other (non-time) correlation extent & form		

Uncertainty PDF shape	MUSICA processing assumes 50% of the uncertainty to be random (normal) and the other 50% to be systematic.	Barthlott et al. (2017)
Uncertainty & units	Modulation efficiency is unitless (assumed uncertainty is 10%) and the phase error unit is rad (assumed uncertainty is 0.1 rad)	Barthlott et al. (2017)
Sensitivity coefficient	Uncertainty propagation according to Eqs. (7) and (8).	
Correlation(s) between affected parameters	Causes positive errors in the retrieved state vector $\hat{x}$ for certain altitudes that are correlated to negative errors at other altitudes (error patterns).	Schneider et al. (2012)
Element/step common for all sites/users?	Yes	MUSICA processing assumes same uncertainties for all sites. These are conservative assumptions.
Traceable to …	Hase (2012)	Modulation efficiency is a relative measurement, e.g. modulation efficiency at maximal optical path difference is related to the modulation efficiency at zero optical path difference.
Validation	Possible, like in Fig. 10. However, the sensitivity of these ILS retrievals has to be documented (like in Fig. 11).	

5.5 Spectroscopic parameters and parameterisations (B3)

Figure 12 depicts measured and simulated spectral microwindows in which H_2O and HDO signatures are dominant. State-of-the-art FTIR spectrometer offer spectra with a very high quality (high spectral resolution together with high signal-to-noise ratios) and small deficiencies in the theoretical description of the spectroscopic signatures can be made visible by analysing the residuals (difference between measured and simulated spectrum) obtained from a retrieval (e.g. Schneider and Hase, 2009).

The middle panel of Fig. 12 shows the residuals when using HITRAN 2008 parameters that are available for a Voigt line shape model. We see systematic residuals in the different microwindows. This strongly suggests that the absorption lines are not correctly described by the HITRAN Voigt line shape parameters. More precisely there must be an inconsistency in the errors of the line intensity parameters. If the relative error in the line intensity parameter

was the same for all lines the spectral fit will correct for this error and it would not become visible in the residuals. However, actually we observe that in some microwindows the residuals are positive and in other microwindows they are negative. This means that the relative line intensity parameter error is very likely different for the different lines. Note that similar residuals are seen across different sites confirming the underlying systematic issue with the lineshape model. Any site-to-site differences are explained by different optical paths through the atmosphere and different atmospheric compositions.

In the bottom panel of Fig. 12 we show the residuals after slightly modifying the line intensity parameters and the line pressure broadening parameters. In addition we considered a speed-dependent Voigt line shape model, i.e. an advanced line shape description model. There are some studies that show the improvement achievable by using such advanced line shape models instead of Voigt line shape models in high resolution infrared remote sensing applications (e.g. Schneider et al., 2011)

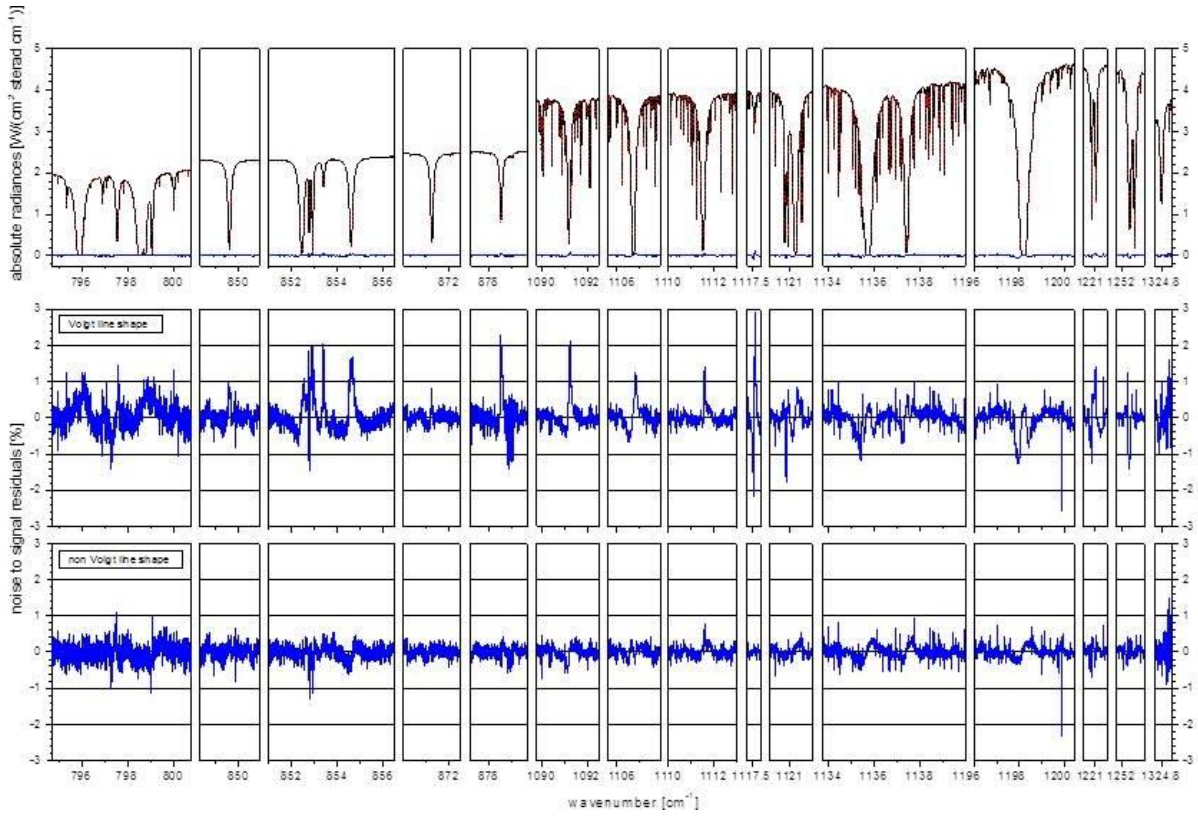

Figure 12. Example of residuals (difference between measured and simulated spectrum) for an H_2O and HDO retrieval that uses different spectral microwindows between 795 and 1325cm^{-1} (the spectrum has been measured at the Izaña Atmospheric Research Centre). Top panel: measured and simulated spectra; Middle panel: residuals achieved when using HITRAN 2008 (Rothman et al., 2009) parameters assuming a Voight line shape model; Bottom panel: residuals achieved when using non-Voigt line shapes.

Information / data	Type / value / equation	Notes / description
Name of effect	Spectroscopy	
Contribution identifier	B3	

Measurement equation parameter(s) subject to effect	Affects vector function $F(x,p)$, the gain matrix **G** and and the Jacobian matrix **K** in Eq. (3)	
Contribution subject to effect (final product or sub-tree intermediate product)	Retrieved state vector $\hat{x}$	
Time correlation extent & form	Systematic	It is a systematic uncertainty
Other (non-time) correlation extent & form		
Uncertainty PDF shape	Normal	
Uncertainty & units	Uncertainty of 1% for the line intensity parameter (absolute unit for line intensity parameter is $cm^{-1}/(mol\ cm^{-2})$: Uncertainty of 1% for the pressure broadening parameter (absolute unit for pressure broadening parameter is cm^{-1} / atm^{-1})	See Barthlott et al. (2017). Furthermore, there are uncertainties by using an inadequate line shape model (see Fig. 12).
Sensitivity coefficient	Uncertainty propagation according to Eqs. (7) and (8)	
Correlation(s) between affected parameters	Causes positive errors in the retrieved state vector $\hat{x}$ for certain altitudes that are correlated to negative errors at other altitudes (error patterns).	Schneider et al. (2012)
Element/step common for all sites/users?	Yes.	
Traceable to …		The inconsistency between the uncertainty of line parameters or parameterisations can be visualised in the differences between simulations and measured high-resolution, high quality spectra (see Fig. 12)
Validation	It is the dominating systematic uncertainty source and can be validated by comparison to reference H2O profile measurements (e.g. Schneider et al., 2016).	

5.6 Solar spectroscopy (B4)

Solar lines are also important in the infrared region. Figure 13 shows the solar transmittance between 750 and 4300cm^{-1} as reported by Hase at al. (2010).

For high quality retrievals it is important to use a high quality atlas of solar lines. However, even then the position and also the strength of the solar line might be different in the measured spectra if compared to the atlas due to a slight mispointing to the centre of the solar disc. A shift in the position is due to a Doppler effect (see explanation in the context of Fig. 9). The solar line strengths will depend on the interaction with the solar atmosphere and will be different for observing the centre or the edge of the solar disc.

The effects of the solar line position can be well accounted for if before a trace gas retrieval the solar line position with respect to the telluric lines is estimated. This can be done by analysing the shifts between two spectral windows. A first window containing a solar line and the second window containing a well understood telluric line (see discussion in the context of Fig. 9).

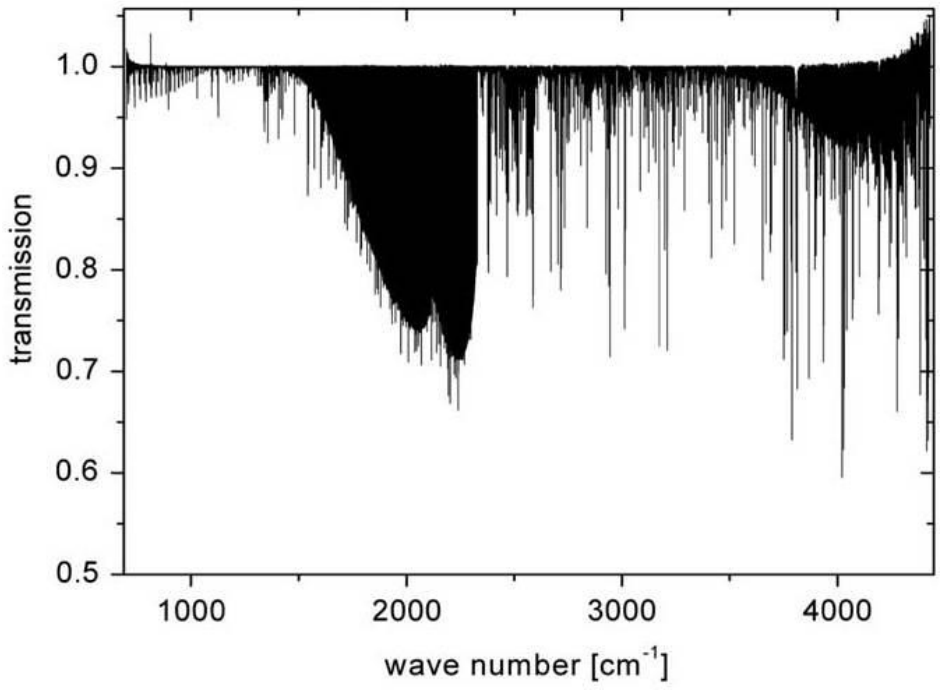

Figure 13. The final ACE-FTS solar transmission spectrum. The apparent bending of the continuum level near the low and high wavenumber ends is actually due to the envelope of increasing noise; the continuum level is constant over the whole region. Adopted from Hase et al. (2010).

Information / data	Type / value / equation	Notes / description
Name of effect	Solar lines	
Contribution identifier	B4	
Measurement equation	Affects vector function	

parameter(s) subject to effect	$F(x,p)$, the gain matrix **G** and and the Jacobian matrix **K** in Eq. (3)	
Contribution subject to effect (final product or sub-tree intermediate product)	Retrieved state vector $\hat{x}$	
Time correlation extent & form	Structured random, similar to B1	
Other (non-time) correlation extent & form		
Uncertainty PDF shape	MUSICA processing assumes 80% random (normal) and 20% systematic.	Barthlott et al. (2017)
Uncertainty & units	Solar line intensity: 1% uncertainty. Solar line ν-scale ($\Delta\nu/\nu$): 10^{-6} uncertainty	Barthlott et al. (2017)
Sensitivity coefficient	Uncertainty propagation according to Eqs. (7) and (8).	
Correlation(s) between affected parameters		
Element/step common for all sites/users?	Yes	MUSICA processing assumes same uncertainties for all sites.
Traceable to …		
Validation	Solar line ν-scale can be validated according to Fig. 9.	

5.7 Atmospheric temperature profile assumptions (B5)

The MUSICA retrievals assume the atmospheric temperature profiles as given by the NCEP (National Centre for Environmental Prediction) reanalyses. The MUSICA tropospheric water vapour retrieval assumes temperature uncertainties for three different altitude ranges (surface - 5km, 5km – 12km, 12km – top of the atmosphere), and no correlation between the uncertainties of the three altitude ranges.

Information / data	Type / value / equation	Notes / description
Name of effect	Temperature	
Contribution identifier	B5	
Measurement equation parameter(s) subject to effect	Affects vector function $F(x,p)$, the gain matrix **G** and and the Jacobian matrix **K** in	

	Eq. (3)	
Contribution subject to effect (final product or sub-tree intermediate product)	Retrieved state vector $\hat{x}$	
Time correlation extent & form	Possible	Could occur if reanalyses data have systematic uncertainties.
Other (non-time) correlation extent & form	Possible	Correlation between different sites are possible if the reanalysis data have correlated uncertainties between different sites.
Uncertainty PDF shape	MUSICA processing assumes 70% random (normal) and 30% systematic.	Barthlott et al. (2017)
Uncertainty & units	3 K (independently for three altitude ranges: surface – 5km; 5km – 12km; 12km – top of atmosphere)	Barthlott et al. (2017)
Sensitivity coefficient	Uncertainty propagation according to Eqs. (7) and (8).	
Correlation(s) between affected parameters	Similar to B2 and B3 error patterns can occur.	
Element/step common for all sites/users?	Yes	MUSICA processing assumes same uncertainties for all sites
Traceable to …	Barthlott et al. (2017)	
Validation	None	

6. Uncertainty Summary

Table 2. Uncertainty Summary.

Element identifier	**Contribution name**	**Typical uncertainty value**	**Effect on final product (error of $\hat{x}$): LT: lower troposphere UT: upper troposphere**	**Traceability level: L/M/H**	**Type**	**Correlated to**
A1	Noise	0.4%	<0.5% (LT) <1.5% (UT)	H	100% random	None
A2	Baseline	0.2%	<8% (LT)	M	50% random and	None

			<15% (UT)		50% systematic	
B1	Pointing	0.1°	<0.05%	H	90% random and 10% systematic	B4
B2	ILS	10% and 0.1 rad	0.6% (LT) 1.5% (UT)	H	50% random and 50% systematic	None
B3	Spectroscopy	1%	<2.5% (LT) <4.5% (UT)	L	100% systematic	None
B4	Solar Lines	1% and 10^{-6}	<0.1%	M	80% random and 20% systematic	B1
B5	Temperature	3 K for 3 independent layers	<1% (LT) <1.5% (UT)	L	70% random and 30% systematic	None

7. Traceability uncertainty analysis

Traceability level definition is given in Table 3.

Table 3. Traceability level definition table

Traceability Level	Descriptor	Multiplier
High	SI traceable or globally recognised community standard	1
Medium	Developmental community standard or peer-reviewed uncertainty assessment	3
Low	Approximate estimation	10

Analysis of the summary table would suggest the following contributions, shown in Table 4, should be considered further to improve the overall uncertainty of the MUSICA H_2O profile product. The entries are given in an estimated priority order. In addition further work would appear warranted to properly quantify the effects currently assumed to add a negligible uncertainty contribution in Figure 6.

Table 4. Traceability level definition further action table.

Element identifier	Contribution name	Typical uncertainty value	Effect on final product (error of $\hat{x}$): LT: lower troposphere UT: upper troposphere	Traceability level: L/M/H	Type	Correlated to
B3	Spectroscopy	1%	<2.5% (LT) <4.5% (UT)	L	100% systematic	None
A2	Baseline	0.2%	<8% (LT) <15% (UT)	M	50% random and 50% systematic	None

B5	Temperature	3 K for 3 independent layers	<1% (LT) <1.5% (UT)	L	70% random and 30% systematic	None

1.1 Recommendations

In order to further improve the traceability of the MUSICA H_2O profile products three priorities have been identified.

The top priority is to quantify rigorously the uncertainty of the simulated spectroscopic signatures (contributor B3). This work must not be limited to the investigation of line intensity and pressure broadening parameters (which are the most important parameters when using a Voigt line shape model). In the meanwhile the ground-based FTIR spectra are of such high quality that a "simple" Voigt line shape parameterisation is very likely not sufficient. It is important to investigate more advanced parameterisations (e.g. Schneider et al., 2011; Tran et al., 2017).

Another priority is to better characterise the baseline distortions for each station individually (contributor A2). This might be achieved by performing regular analyses of black body radiances by the whole observing system (solar tracker unit and FTIR spectrometer). However, such calibration measurements can hardly be automated and would need more manpower.

Finally, the atmospheric temperature uncertainty (contributor B5) should be better characterised for each individual site. This should be done in collaboration with providers of reanalyses data that are used as the atmospheric temperature in the MUSICA H_2O retrievals.

In addition to improved assessment of the key uncertainty contributors described above further work could be undertaken to quantify and assess the nature of the uncertainties from the other (assumed minor) contributors from the other elements identified in the overall product traceability and uncertainty chain (Figure 6).

8. Conclusions

The MUSICA H_2O profile product has been assessed against the GAIA CLIM traceability and uncertainty criteria.

9. References

Barthlott et al. (2017), doi:10.5194/essd-9-15-2017.
Davis et al. (2001), ISBN 0-12-042510-6.
Gisi et al. (2011), doi:10.5194/amt-4-47-2011.
Hase (2000), Dissertation, FZK Report No. 6512, Forschungszentrum Karlsruhe, Germany.
Hase et al. (2010), doi:10.1016/j.jqsrt.2009.10.020.
Hase (2012), doi:10.5194/amt-5-603-2012
Rodgers (2000), ISBN 981-02-2740-X.
Rothman et al. (2009), doi:10.1016/j.jqsrt.2009.02.013.
Schneider and Hase (2009), doi:10.1016/j.jqsrt.2009.04.011.
Schneider et al. (2011), doi:10.1016/j.jqsrt.2010.09.008.
Schneider et al. (2012), doi:10.5194/amt-5-3007-2012.
Schneider et al. (2016), doi:10.5194/amt-9-2845-2016.
Tran et al. (2017), doi:10.1063/1.4983397.